Int J Adv Manuf Technol (2006) 28: 665–670
DOI 10.1007/s00170-004-2423-x

ORIGINAL ARTICLE

Ta-Shi Lai

Design and machining of the epicycloid planet gear of cycloid drives

Received: 20 July 2004 / Accepted: 18 September 2004 / Published online: 27 April 2005

Abstract This paper presents a mathematical model and design procedures to design the epicycloid planet gear of cycloid drives. It is based on coordinate transformation, envelope theory, and theories of conjugate surfaces, from which the equation of meshing is derived, while the path of machining tools is obtained by the equidistant curve principle. In addition, a program is developed to solve the equations of meshing and conjugate surfaces. Therefore, the epicycloid-profile is obtained. Then, these data are used to construct the 2D drawing and solid modeling of the epicycloid-planet-gear using AutoCAD and Pro/E (a CAD software package), respectively. The CAD data is used for machining, in this case by a wire-cutting machine. The manufactured component is presented to demonstrate that the design procedures and manufacturing are feasible. The design approach and machining method are suitable for applying CAD and CAM in industrial fields.

Keywords CAD · Cycloid drives · Geometric design · Solid modeling

1 Introduction

Cycloid drives have been popular reducers from the 1930s until the present time due to their compact, light-weight, high speed reduction compared to planetary gear trains, together with their high mechanical advantage in a single stage [1]. The cycloid drive has been used widely in industry for speed, torque conversion purposes, and precision pointing; since in these applications it has high efficiency, high speed ratios, and compactness in a single stage. However, there is backlash in the cycloid drive due to variations in machining, which will reduce stability and inherent noise and vibration, particularly at high speeds [2]. If a cycloid drive were manufactured to the ideal dimensions, there would be no backlash, so manufacturing precision is very important in cycloid drive machining. One key part of the cycloid drives, the epicycloid planet gear, has complex-shaped surfaces, which must be manufactured by non-traditional machining such as EDM, CNC machine or other modern machining methods [3]. Furthermore, for a complex component it is best to use powerful information tools and advanced techniques. This paper presents the results of work on one such approach to geometric and computer-aided design and manufacturing.

The geometry of conjugate surfaces is of major concern in designing the gears and generating the conjugate meshing elements, and the meshing of gears and the generations of conjugate surfaces have been previously studied [4–8]. The envelope theory has been applied to gear drives or meshing elements [9–12]. Litvin and Feng [13] used differential geometry to generate the conjugate surfaces of cycloidal gearing. Sung and Tsai [14] studied contact ratios of extended cycloid and cycloid bevel gear sets. Liang and Liu [15] studied the mathematical model and undercutting analysis of The epitrochoid gear for the cycloid drives.

This paper provides the design and manufacturing procedures for the epicycloid planet gear of cycloid drives. Below, we present the topological structure of the cycloid drive, and determine coordinate systems and coordinate transformation matrices. Then, the equation of meshing is derived based on the fundamental gearing kinematics, coordinate transformation, envelope theory, and the theory of conjugate surfaces. In addition, the equidistant curve principle is used to obtain the path for machining tools. Using computer-aided design (CAD) the drawing of the epicycloid planet gear while solid modeling is constructed and presented. Finally, the design data are used for the machining of wire cutting and the manufactured component.

2 Topological structure

Figure 1 shows the topological structure of the cycloid drive. Member 2 is a ring gear, which has cylindrical rollers as its teeth, and is composed of member 2a (ring gear) and member

T.-S. Lai
Department of Vehicle Engineering,
National Huwei University of Science & Technology,
Huwei, Yuenlin 63208, Taiwan
E-mail: tslai@ sunws.nhust.edu.tw
Fax: +886-5-6321571

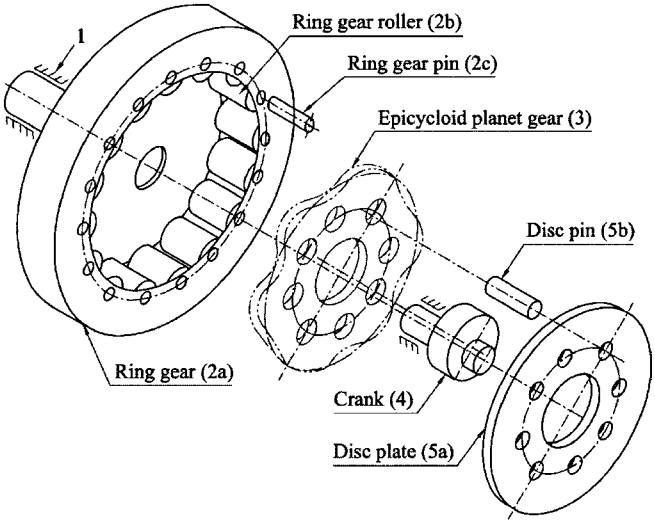

Fig. 1. Topological structure of the cycloid drive

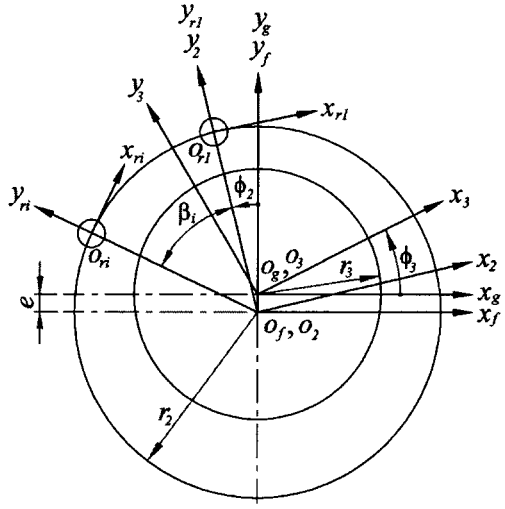

Fig. 3. Coordinate systems

2b (cylindrical roller). Member 3 is an epicycloid planet gear in which its profiles are generated by ring gear rollers (teeth). Member 4 is a crank. Member 5b (disc pin) is a floating connection with member 3a and member 5a (disc plate). Members 5a and member 5b are together treated as member 5. This mechanism employs a crank (member 4) to devote the epicycloid planet gear (member 3) that orbits about the center of the input shaft due to the eccentricity of the shaft. At the same time, the epicycloid plane gear rotates about its own center, in the opposite direction of the input shaft, due to the engagement with the ring gear (member 2). The disc pins (member 5b) are floating connections with the epicycloid planet gear and the disc plate (member 5a). The disc plate, rotating in the same direction as the epicycloid planet gear, is the output.

The topological structure of this cycloid drive is shown in Fig. 2a. It consists of five members: the frame (member 1), the ring gear (member 2), the epicycloid planet gear (member 3), the crank (carrier, member 4), and the disc plate (member 5). The joints between the frame and the ring gear, the frame and the crank, the frame and the disc plate, and the epicycloid-planet-gear and the crank are revolute pairs. The ring gear and the epicycloid planet gear are incident to a gear pair, whereas the epicycloid planet gear and the disc plate are incident to a cam pair. In order to design the conjugate surfaces of the cycloid drive, this five-link and six-joint mechanism is modeled kinematically into a three-link and three-joint mechanism as shown in Fig. 2b. Only links 1, 2, and 3 are considered in the geometry analysis of this cycloid drive.

3 Coordinate systems

Before deriving the surface equation of the ring gear of the proposed cycloid drive, coordinate systems corresponding to the cycloid drive should be defined. The coordinate systems of the cycloid drive are shown in Fig. 3. The fixed coordinate systems $(xyz)_f$ and $(xyz)_g$ are rigidly connected to the frame. The moving coordinate systems $(xyz)_2$, $(xyz)_{ri}$, and $(xyz)_3$ are rigidly connected to the ring gear, the ith cylindrical roller, and the epicycloid-planet-gear, respectively. The ring gear rotates about the z_2 axis with a constant angular velocity. The epicycloid planet gear rotates about the z_3 axis. The moving coordinate system $(xyz)_{ri}$ attached to the ith cylindrical roller is set up and angle β_i is comprised between y_{r1} and y_{ri} axes. Origins o_f and

Fig. 2. Skeletons of the cycloid drive

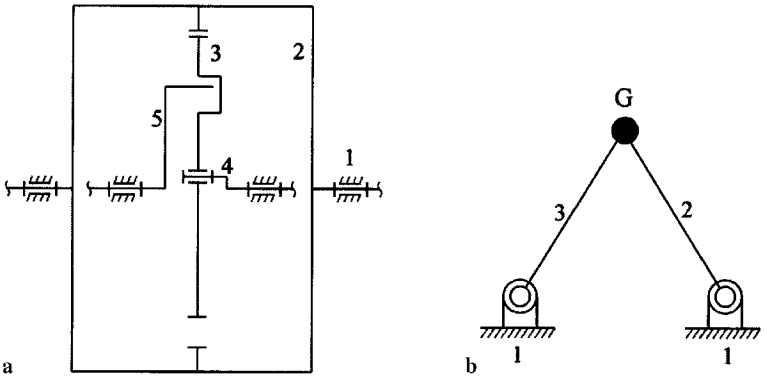

Fig. 4. The cylindrical roller

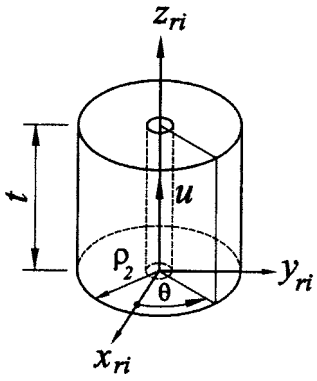

o_2 are coincident and located at the center of the ring gear while origins o_g and o_3 are coincident and located at the center of the epicycloid-planet-gear. Origin o_{ri} is coincident and located at the center of the ith cylindrical roller base surface. Axis x_f is parallel with axis x_g. The directions of axes z_f, z_g, z_2, z_3, and z_{ri} are perpendicular to the xy plane. Angles ϕ_2 and ϕ_3 are the angular displacements of the ring gear and the epicycloid-planet-gear, respectively. Positive ϕ_2 and ϕ_3 are measured counterclockwise with respect to axis z_2 and axis z_3, respectively. The distance between the axes of rotation of the ring gear and the epicycloid planet gear is e. The distance between the center of the ring gear and the center of the teeth of ring gear is r_2. We assume the epicycloid planet gear has a phantom radius r_3. The coordinate system of the cylindrical roller is shown in Fig. 4. The cylindrical roller of the ring gear is a circle of radius ρ_2. The height of the cylindrical roller of the ring gear is t.

4 Coordinate transformation matrices

According to the definition of all parameters and coordinate systems, we have the following transformation matrices of the coordinate systems by applying homogeneous coordinates and 4×4 matrices for coordinate transformation [16, 17]. By transforming the coordinate systems from $(xyz)_{ri}$ to $(xyz)_3$, the transformation matrix can be expressed as:

$$\mathbf{M}_{3,ri} = \begin{bmatrix} \cos(\phi_3-\phi_2-\beta_i) & \sin(\phi_3-\phi_2-\beta_i) & 0 & r_2\sin(\phi_3-\phi_2-\beta_i)-e\sin\phi_3 \\ -\sin(\phi_3-\phi_2-\beta_i) & \cos(\phi_3-\phi_2-\beta_i) & 0 & r_2\cos(\phi_3-\phi_2-\beta_i)-e\cos\phi_3 \\ 0 & 0 & 1 & 0 \\ 0 & 0 & 0 & 1 \end{bmatrix} \tag{1}$$

where, matrix $\mathbf{M}_{i,j}$ represents the transformation matrix from system j to system i.

In homogeneous coordinates, the position vector $\mathbf{P}$ can be represented as:

$$\mathbf{P} = \begin{bmatrix} p_x & p_y & p_z & 1 \end{bmatrix}^T \tag{2}$$

where, p_x, p_y, and p_z are the components of position vector $\mathbf{P}$ in x, y, and z, respectively, and superscript "T" means transposition. In coordinate system $(xyz)_{ri}$, for the ring gear with cylindrical rollers, the homogeneous coordinates position vector of the ith cylindrical roller of the ring gear can be expressed as:

$$\mathbf{R}_{ri} = \begin{bmatrix} \rho_2\cos\theta & \rho_2\sin\theta & u & 1 \end{bmatrix}^T \tag{3}$$

where $0 \le \theta \le 2\pi$, $0 \le u \le t$, and $\mathbf{R}_i$ denotes the surface equation in coordinate system i. By transforming the equation of the ring-gear cylindrical roller coordinate systems from $(xyz)_{ri}$ to $(xyz)_3$, the surface equation of the cylindrical rollers of the ring gear can be expressed as:

$$\mathbf{R}_3^{ri} = \mathbf{M}_{3,ri}\mathbf{R}_{ri} = \begin{bmatrix} \rho_2\cos(\phi_3-\phi_2-\beta_i-\theta)+r_2\sin(\phi_3-\phi_2-\beta_i)-e\sin\phi_3 \\ -\rho_2\sin(\phi_3-\phi_2-\beta_i-\theta)+r_2\cos(\phi_3-\phi_2-\beta_i)-e\cos\phi_3 \\ u \\ 1 \end{bmatrix} \tag{4}$$

where $\mathbf{R}_j^i$ denotes the ith surface equation in coordinate system j.

Letting gear ratio $m = \phi_3/\phi_2$ and $\phi = \phi_2$, then Eq. 4 becomes:

$$\mathbf{R}_3^{ri} = \begin{bmatrix} \rho_2\cos[(m-1)\phi-\beta_i-\theta]+r_2\sin[(m-1)\phi-\beta_i]-e\sin(m\phi) \\ -\rho_2\sin[(m-1)\phi-\beta_i-\theta]+r_2\cos[(m-1)\phi-\beta_i]-e\cos(m\phi) \\ u \\ 1 \end{bmatrix} \tag{5}$$

where ϕ is the generated parameter of motion, angles ϕ and β_i are the parameters of the family, and θ and u are parameters on the particular surface of the family.

5 Equation of meshing and path of machining tools

In order to obtain the epicycloid profile, the cycloid drive must be determined by the conjugate surface that satisfies specific conjugate relations, and the theory of differential geometry is applied to find the equation of meshing [17]. Consider coordinate systems $(xyz)_2$, $(xyz)_{ri}$, $(xyz)_3$, and $(xyz)_f$ that are connected to the ring gear, the ith cylindrical roller, the epicycloid planet gear, and the frame, respectively. When u and θ are the parameters of the tooth-profile, the ith cylindrical roller of the ring gear is provided with a regular surface Σ_{ri} that is represented in coordinate system$(xyz)_3$ as follows:

$$\mathbf{R}_{ri}(u,\theta),\ \frac{\partial \mathbf{R}_{ri}}{\partial u} \times \frac{\partial \mathbf{R}_{ri}}{\partial \theta} \neq \mathbf{0} \tag{6}$$

The gears must transform prescribed motions being in line contact at every instant. The location and orientation of gear axes and function $\phi_3(\phi_2)$ are given. Here, ϕ_2 and ϕ_3 are the angles of rotation of the ring gear and epicycloid-planet-gear, respectively. The required type of contact of epicycloid-planet-gear tooth (epicycloid profiles) surfaces can be provided if the tooth surface of the ring gear is determined as the envelope to the family of surfaces, Σ_ϕ, that is generated in coordinate system $(xyz)_3$ by surface Σ_{ri}.

Now, we consider the necessary and sufficient conditions of the existence of surface Σ_3. The necessary conditions of existence

for surface Σ_3 provide that surface Σ_3 (if it exists) is in tangency with surface Σ_{ri}. The sufficient conditions of existence of surface Σ_3 provide that surface Σ_3 is indeed in tangency with surface Σ_{ri}, and that surface Σ_3 is a regular surface. From the necessary conditions of existence of surfaces viewpoint, the ring gear has the cylindrical roller that is a ruled developable surface. Therefore, envelope theory can be applied to deal with the equation of meshing [17, 18]. From envelope theory for a one-parameter family of surfaces, the equation of meshing is obtained as follows:

$$\left(\frac{\partial \mathbf{R}_3^{ri}}{\partial u} \times \frac{\partial \mathbf{R}_3^{ri}}{\partial \theta}\right) \cdot \frac{\partial \mathbf{R}_3^{ri}}{\partial \phi} = 0 \tag{7}$$

Equation 7 relates the curvilinear coordinates (u, θ) of surface Σ_{ri} with the generalized parameter of motion, ϕ.

By differentiating Eq. 5 with respect to u, θ, and ϕ, respectively, we obtain:

$$\frac{\partial \mathbf{R}_3^{ri}}{\partial u} = \begin{bmatrix} 0 & 0 & 1 & 0 \end{bmatrix}^T \tag{8}$$

$$\frac{\partial \mathbf{R}_3^{ri}}{\partial \theta} = \begin{bmatrix} \rho_2 \sin[(m-1)\phi - \beta_i - \theta] \\ \rho_2 \cos[(m-1)\phi - \beta_i - \theta] \\ 0 \\ 0 \end{bmatrix} \tag{9}$$

$$\frac{\partial \mathbf{R}_3^{ri}}{\partial \phi} = \begin{bmatrix} -\rho_2(m-1)\sin[(m-1)\phi-\beta_i-\theta] + r_2(m-1)\cos[(m-1)\phi-\beta_i] - em\cos(m\phi) \\ -\rho_2(m-1)\cos[(m-1)\phi-\beta_i-\theta] - r_2(m-1)\sin[(m-1)\phi-\beta_i] - em\cos(m\phi) \\ 0 \\ 0 \end{bmatrix} \tag{10}$$

Substituting Eqs. 8, 9, and 10 into Eq. 5, we have:

$$\tan\theta = \frac{-r_2(m-1) + em\cos(\phi + \beta_i)}{em\sin(\phi + \beta_i)} \tag{11}$$

Equation 11 is called the equation of meshing, which provides two solutions for consideration, given ϕ, and provides two solutions for θ that differ by 180°.

In order to obtain the path for machining tools of the epicycloid profiles, the equidistant curve principle is applied to generate the equidistant curves of the epicycloid profiles. Figure 5 shows c_1 and c_2 for the epicycloid curve and its equidistant curve, respectively. Let the points $p_1(x_c, y_c)$ and $p_2(x_p, y_p)$ lie on c_1 and c_2, respectively. The direction of the tangent line at point p_1 is τ. The direction of the line n, between points p_1 and p_2, is perpendicular τ. From the geometry of Fig. 5, the relationship between these curves can be expressed as follows:

$$(x_p - x_c)^2 + (y_p - y_c)^2 = s^2 \tag{12}$$

$$f'(x_c) \cdot \frac{y_p - y_c}{x_p - x_c} = -1 \tag{13}$$

Equation 12 is the equation of distance between the epicycloid profile and its equidistant curve. Here, s is the distance between points p_1 and p_2. Equation 13 represented that the tangent line at the epicycloid profile is perpendicular to the line between points p_1 and p_2. The term $f'(x_c)$ represents the differential for

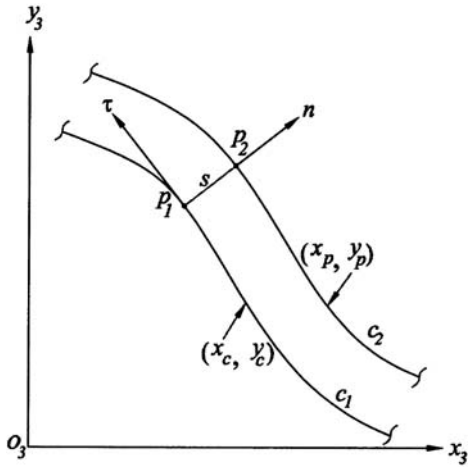

Fig. 5. Equidistant curve

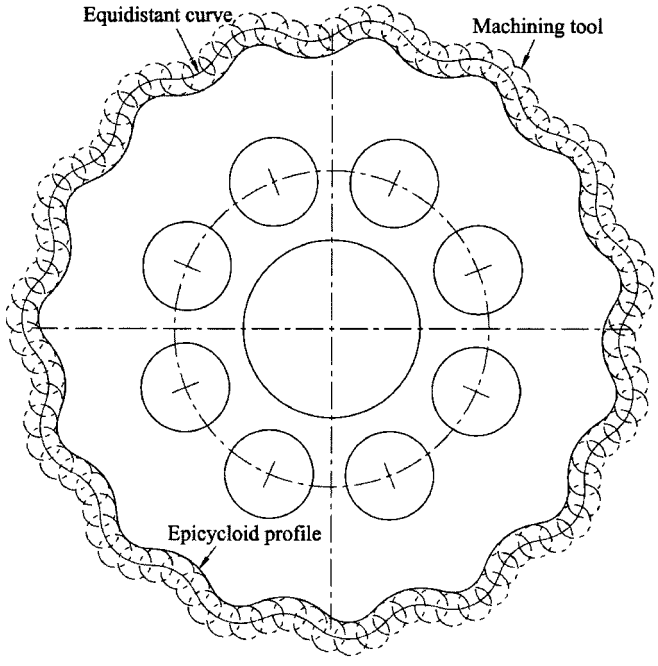

Fig. 6. The path of machining tools

epicycloid profiles. Simultaneously solving Eqs. 12 and 13, the equidistant curve of the epicycloid profile can be obtained when the distance s is specified, therefore the path for machining tools is obtained as shown Fig. 6. The equidistant curve is the reference profile of the machining tools.

6 Numerical example

To avoid interference in gear driving, the equation of meshing must be considered. The envelope of surface Σ_3 to the family surface of cylindrical roller is determined with Eqs. 5 and 11 considered simultaneously. The envelopes are called the conju-

gate surfaces of the ring-gear-roller. A computer program is developed to solve the equations of meshing and surface; and then CAD uses the resulting data to automatically generate the epicycloid profile. Figures 7 and 8 show the 2D drawing epicycloid profile and solid modeling of the epicycloid-planet-gear, respectively, for a speed ratio equal to 15, $r_2 = 60$ mm, $Z_2 = 16$, $Z_3 = 15$, $e = 2$ mm, $\rho_2 = 9$ mm, $\beta_i = 0$, $t = 8$ mm, and $0 \le \phi \le 2\pi$. Where Z_2 and Z_3 denoted the number of the ring-gear rollers, the number of the epicycloid-planet-gear teeth (the number of the epicycloid-profile lobes), respectively. Using AutoCAD and Pro/ENGINEER (a CAD package software) construct the 2D drawing and solid modeling, respectively.

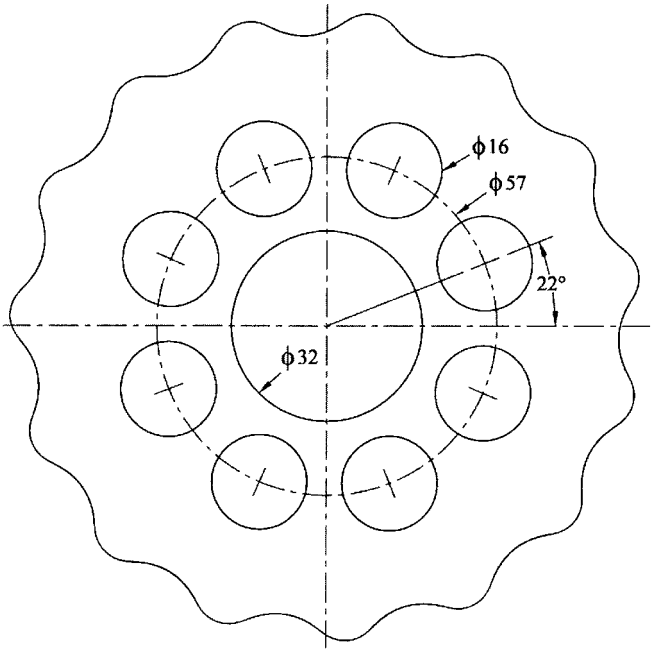

Fig. 7. Drawing of the epicycloid planet gear

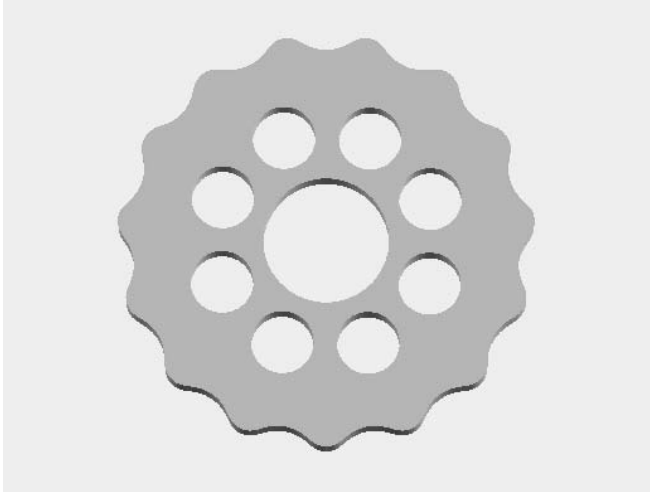

Fig. 8. Solid modeling of the epitrochoid planet gear

7 Implementation

Simple-shaped components can be manufactured using conventional machines in large batches or using group technology, but for complex contour components it is best to use powerful information tools and an advanced approach. Because the epicycloid-profile is a complex surface, it must be manufactured on a CNC machine or other modern machining method, so it is necessary to select powerful modern technology for the design and manufacturing. We have therefore proposed an electrical discharge wire cutting as the machining method, which fulfils the requirement of manufacturing precision. These CAD data, in DXF or other file, can be interpreted by machining codes for the CNC EDM machine. The machining of hardened steel using electrical discharge machining (EDM) eliminates the need for subsequent heat treatment which has the possibility of distortion.

The billet material is SKD-11 cut from a plate, and the first sequence is heat treatment. This work piece is then placed in

Fig. 9. The epicycloid planet gear during manufacture

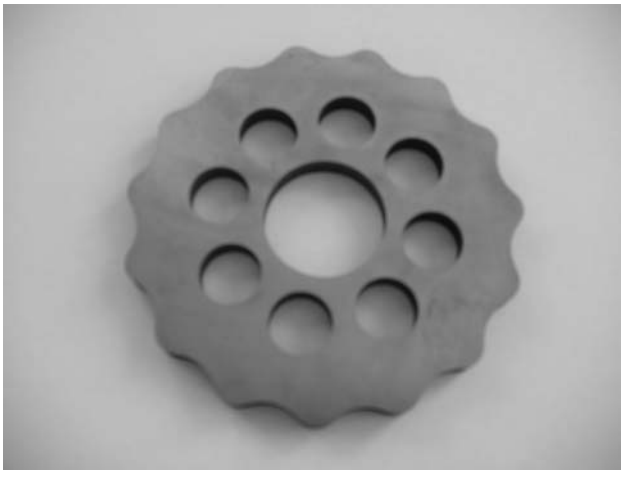

Fig. 10. The manufactured epicycloid planet gear component

the traveling wire EDM machine (EDM wire cutting machine in this case) for manufacturing. The EDM wire-cutting machine is a Mitsubishi electrical discharge machine unit, Model FX2. The data, in a drawing constructed by AutoCAD constructing as shown Fig. 7, are the tool path codes and cutter location data that were created in the DXF file of AutoCAD. Figures 9 and 10 show the epicycloid planet gear during and after machining, respectively.

8 Conclusions

This paper presents the results of work on one such approach to computer-aided design and manufacturing, and derives the surface equation of a cycloid drive using envelope theory to deal with the equation of meshing. We further develop a program to solve the meshing and surface equations that can design required speed ratios of the cycloid drive. Using this design and manufacturing procedure is an effective approach for cycloid drive manufacturing. It is also an advanced approach for improving conventional design and manufacturing. This approach not only increases design efficiency but also can improve the machining precision, thus reducing the noise and backlash of the cycloid drives. A 2D drawing, a solid modeling, and a photograph of manufactured component are presented to demonstrate the feasibility of this approach.

Acknowledgement The author is grateful to the National Science Council of the Republic of China (Taiwan) for supporting this research under grant NSC 91-2212-E-150-027.

References

1. Botsiber DW, Kingston L (1956) Design and performance of cycloid speed reducer. Mach Des June:407–414
2. Blanche JG, Yang DCH (1989) Cycloid drives with machining tolerances. J Mech, Transm, and Automat Des 111:337–344
3. ASM International Handbook Committee (1989) Metals handbook ninth edn vol 16 machining. ASM International, Metal Park, OH
4. Litvin FL (1968) The synthesis of approximate meshing for spatial gears. J Mech 3:131–148
5. Tsai YC, Chin PC (1987) Surface geometry of straight and spiral bevel gears. ASME Trans, J Mech, Transm, Automat Des 109:443–449
6. Lin CC, Tsai LW (1993) The trajectory analysis of bevel gear Trains. ASME Trans, J Mech Des 115:164–170
7. Yan HS, Liu JY (1993) Geometric design and machining of variable pitch lead screws with cylindrical meshing elements. ASME Trans,J Mech Des 115(4):490–495
8. Yan HS, Lai TS (2002) Geometry design of an elementary planetary gear train with cylindrical tooth-profiles. Mech Mach Theory 37(6):757–767
9. Hanson DRS, Churchill FT (1962) Theory of envelope provided new CAM design equation. Prod Eng Aug:45–55
10. Colbourne JR (1974) The geometry of trochoid envelopes and their application in rotary pumps. Mech Mach Theory 4:421–435
11. Litvin FL, Kin V (1992) Computerized simulation of meshing and bearing contact for single-enveloping worm-gear drives. ASME Trans, J Mech Des 114:313–316
12. Tsay DM, Hwang GS (1994) Application of the theory of envelope to the determination of camoid profiles with translating followers. ASME Trans, J Mech Des 116:320–325
13. Litvin FL, Feng PH Computerize design and generation of cycloidal gearing. Mech Mach Theory 31:891–911
14. Sung LM, Tsai YC (1997) A study on the mathematical models and contact ratios of extended cycloid and cycloid bevel gear sets. Mech Mach Theory 32(1):39–50
15. Liang S, Liu JY (2000) Mathematical model and undercutting analysis of epitrochoid gear for the cycloid drives. In: Su D (ed), International Conference on Gearing, Transmissions and Mechanical Systems. Professional Engineering Publishing, London, pp 293–303
16. Denavit J, Hartenberg RS (1955) A kinematic notation for lower pair mechanisms base on matrices. ASME Trans, J Appl Mech 22(2):215–221
17. Litvin FL (1994) Gear geometry and applied theory. Prentice-Hall, Englewood Cliffs, NJ
18. Goetz A (1970) Introduction to differential geometry. Addison-Wesley, Boston, MA

Nomenclature

e	Distance between the centers of ring gear and epicycloid-planet-gear
$\mathbf{M}_{i,j}$	Coordinate transformation matrix from system j to system i
r_2	Radius of ring gear
t	Tooth height of ring gear
Z_2	Tooth number of the ring gear
Z_3	Tooth number of the epicycloid-planet-gear
$\mathbf{R}_i$	Surface equation in coordinate system i
$\mathbf{R}_j^i$	The ith surface equation in coordinate j
u, θ	Curvilinear coordinates on the surface of the meshing ring gear
$(xyz)_2$	Moving coordinate system rigidly connected to the ring gear
$(xyz)_3$	Moving coordinate system rigidly connected to the epicycloid-planet-gear
$(xyz)_f$	Fixed coordinate system rigidly connected to the frame at point f
$(xyz)_g$	Fixed coordinate system rigidly connected to the frame at point p
$(xyz)_{ri}$	The ith moving coordinate system rigidly connected to the ith cylindrical roller of the ring gear
β_i	Angle between the first cylindrical roller and the ith cylindrical roller of the ring gear
ϕ_2	Angular displacement of ring gear
ϕ_3	Angular displacement of epicycloid-planet-gear
Σ_2	Ring gear surface
Σ_{ri}	The ith cylindrical roller surface of the ring gear
ρ_2	Radius of cylindrical roller of the ring gear